Period -control in a coupled system of two genetic oscillators for synthetic biology

Eleni Firippi, Madalena Chaves

This is a preliminary version of the article published at:
8th IFAC Conference on Foundations of Systems Biology in Engineering (Valencia, Spain), 2019.

Period - control in a coupled system of two genetic oscillators for synthetic biology

Eleni Firippi and Madalena Chaves*

November 28, 2019

Abstract

Biological complex mechanisms with oscillatory behavior are often modeled by high dimensional nonlinear ODEs systems, which makes the analysis and understanding the dynamics of the system difficult. In this work, we consider two reduced models that mimic the oscillatory dynamics of the cell cycle and the circadian clock, and study their coupling from a synthetic biology perspective. To improve the performance and robustness of the oscillatory dynamics in a living cellular environment, we consider the problem of augmenting the parameter region admitting periodic solutions. Moreover, we study the capacity for mutual period regulation and control of the coupling between the two reduced oscillators.

1 Introduction

Biological oscillators often involve a complex network of interactions, as in the case of circadian rhythms or cell cycle. Mathematical modeling and especially model reduction help to understand the main mechanisms behind oscillatory behavior. Low dimensional systems can be found at the core of oscillatory dynamics, such as a basic 3-dimensional negative feedback loop or a 2-dimensional negative loop with self-regulation (Smolen et al. (1998)). Moreover, both of these systems have been synthetically constructed in living cell environment and indeed shown to oscillate (Elowitz and Leibler (2000), Stricker et al. (2008), Purcell et al. (2010)).

A new challenge in synthetic biology is to study the behavior of an oscillator when coupled to another system (Tomazou et al. (2018), Perez-Carrasco et al. (2018)). Interesting questions include the tuning capacity and period control for the coupled system. In this context, we perform a model-based investigation for the coupling between two oscillators, mimicking the cell cycle and circadian clock. This analysis aims to contribute to gain further intuition on the interactions between these oscillators (Feillet et al. (2015)) and their mutual regulation of the period of oscillations.

A simple model proposed by Smolen et al. (1998), consists of two *transcriptional factors* that compete with each other in a negative feedback loop, possibly generating oscillatory behavior. Such a system is able to describe complex autonomous mechanisms like the *circadian clock*, in terms of their function and properties, i.e. oscillatory behavior, feedback, autoregulation of the transcriptional factors.

To characterize the region of parameters which admits sustained oscillations for the Smolen model, we first compute numerically the limit cycle solutions of the system as a function of its parameters, and then propose one way to increase the region of sustained oscillations.

*The authors are with Université Côte d'Azur, Inria, INRA, CNRS, Sorbonne Université, Biocore team, Sophia Antipolis, France. The authors were partly supported by the French national agency for research through project ICycle ANR-16-CE33-0016-01.

A two-dimensional model for the cell cycle was recently proposed by Almeida et al. (2017). It represents the concentration of cyclin B and a complex APC that promotes exit from mitosis. This model was calibrated from experimental data and its region of oscillations can also be characterized in terms of the parameters.

A short outline of this paper is as follows: in Sections 2 and 3 we introduce the two models with an improved version of Smolen oscillator. Section 4 contains the coupling schemes for the two models. Section 5 explores the coupled system dynamics and its period response. Lastly, in Section 6 we give an overall view of our results and some aspects for their application in synthetic biology.

2 Two genetic oscillators

In gene regulatory networks, the molecular links between the components of the network can be expressed through a system of ODEs: $\dot{x_i} = f_i(x_1, \ldots, x_n)$, where the f_i depend on the nodes that have an effect on proteins concentrations $x_i, \in [0, +\infty)$, $i = 1, \ldots, n$ of the gene i. The most common forms of interactions are: binding or unbinding of two molecules, inhibition, activation and degradation. These interactions can be translated into mathematical expressions based on *mass-action* laws, *saturation* or Hill functions.

2.1 The Smolen oscillator

The two dimensional model introduced in Smolen et al. (1998) is composed of two transcription factors *TF-A* and *TF-R* and models a negative feedback circuit of a form that appears for instance in the mechanism of the circadian clock: TF-A is a transcriptional activator that can bind to responsive elements DNA sequences (REs) and TF-R is a protein that represses transcription by competing with TF-A for binding to REs. Besides the core negative feedback loop there are also additional negative and positive autoregulations to the activator and the repressor. For simplicity, *TF-A* and *TF-R* are denoted A and R respectively. Considering that A activates both components and R represses both components in a similar way the model of the oscillator becomes:

$$\begin{aligned} \frac{dA}{dt} &= V_A \frac{A^2}{A^2 + \theta_0(1 + R/\theta_2)} - \gamma_A A + r_{bas} \\ \frac{dR}{dt} &= V_R \frac{A^2}{A^2 + \theta_1(1 + R/\theta_2)} - \gamma_R R \end{aligned} \tag{1}$$

The parameters V_A, $V_R > 0$ express the synthesis rate of the two transcriptional factors and are measured in min^{-1}. The degradation rate parameters γ_A, $\gamma_R > 0$ are also measured in min^{-1}. The concentration and activity thresholds θ_0, θ_1, $\theta_2 > 0$ are considered to be dimensionless. For the parameter set given by Smolen et al. (1998) (we call it p_S) the model has a periodic solution.

System (1) is a good candidate for implementation in synthetic biology, due to its reduced dimension. One version of this oscillator was indeed implemented using the gene lacI as a repressor and araC as an activator (see Stricker et al. (2008), Purcell et al. (2010)). However, in a neighbourhood of p_S, the region of parameters where oscillations are observed is rather small. In this study, our first goal is to better understand the effect of each parameter in generating oscillations, and propose a more efficient design.

Three alternative cases for the model have been explored with the objective of improving the design of system (1), such that periodic solutions are observed for a larger region of the parameter set: (a) eliminating the autoregulation of the repressor (negative self-loop on R), (b) eliminating the autoregulation of the activator (positive self-loop on A) and (c) eliminating both self-loops. From our analysis and simulations only the first case (a) appeared to admit periodic solutions.

Table 1: Parameters of improved Smolen model

$V_A = 12.5\ min^{-1}$	$V_R = 0.3\ min^{-1}$
$\gamma_A = 1\ min^{-1}$	$\gamma_R = 0.2\ min^{-1}$
$\theta_0 = 10$	$\theta_1 = 16$
$r_{bas} = 0.4\ min^{-1}$	$\theta_2 = 0.2$

2.2 An improved Smolen oscillator

Figure 1: Smolen oscillator with activator autoregulation.

If the self-inhibition loop on R is removed the system (1) becomes:

$$\begin{aligned} \frac{dA}{dt} &= V_A \frac{A^2}{A^2 + \theta_0(1 + R/\theta_2)} - \gamma_A A + r_{bas} \\ \frac{dR}{dt} &= V_R \frac{A^2}{A^2 + \theta_1} - \gamma_R R \end{aligned} \tag{2}$$

In the next paragraphs, we will compare the dynamics of the original system (1) with the alternative (2). Using the numerical toolbox Matcont for MATLAB Dhooge et al. (2003) we perform bifurcation analysis for the model parameters.

First, we performed bifurcation analysis for the activator synthesis rate parameter V_A, for the original model (1) and case (2), shown in Fig. 2. Comparing the results we observe that the interval in which periodic solutions exist for the system, increased significantly for the case (2): the length of the interval increased by a factor 6. A second observation is that the amplitude of the limit cycle increased -approximately doubled- for (2).

We also perform a two parameter bifurcation analysis for the remaining parameters of (1) and (2). The results are in an agreement with the one parameter analysis regarding the increase of the oscillations interval. From the comparison we conclude that removing the autoregulation of the repressor increases the parameter region where oscillations exist, by approximately doubling the range allowed for each parameter.

We further analyse the system (2) in the context of the piecewise affine formalism (PWA), introduced by Glass and Kauffman (1973), and we obtain certain conditions for its parameters. In particular, a closer look in the analysis of the PWA system, shows that requiring $\sqrt{\theta_1} > \sqrt{\theta_0}$, see Table 1, we can compute the first return map of the PWA system and prove that it has a unique fixed point which is unstable, Firippi and Chaves (In preparation).

To establish now that (2) can be interpreted as a minimal mammalian clock model we consider that the activator A represents the fundamental protein BMAL1 which activates the transcription of several clock proteins, including REV-ERBα, PER and CRY. In turn, there is also an auxiliary loop of REV-ERBα which inhibits BMAL1 making it a good candidate for the repressor R. The proteins CRY and PER form a complex (PC) which binds to BMAL1 to inhibit the transcription of genes that are regulated by CLOCK-BMAL1, as well as their own transcription (autoregulation) Ye et al. (2014). Describing in a simplified way, BMAL1 and PC mutually inhibit each other's activities by binding. The positive self-regulation of A can be interpreted as the result of this double negative loop.

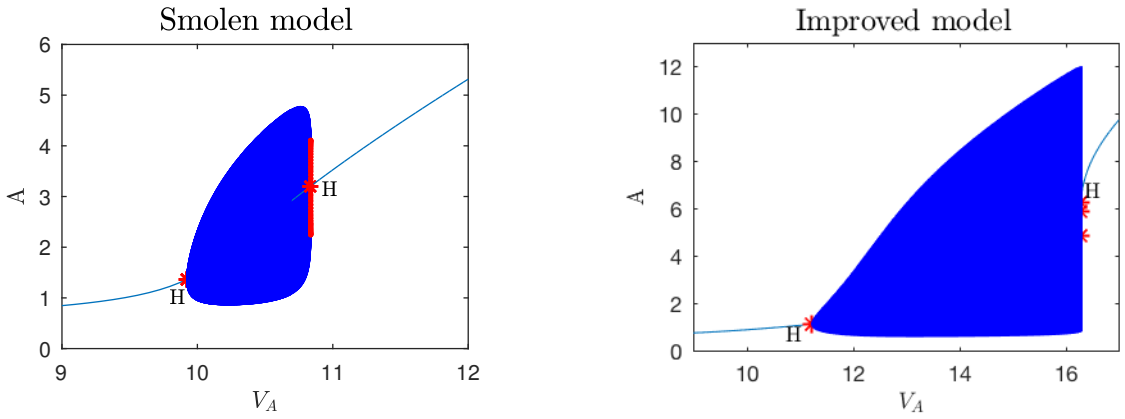

Figure 2: Bifurcation analysis for the V_A parameter (synthesis rate of A) and the the amplitude of the limit cycle, for the two systems, the Smolen model and case (2). The red stars indicate critical Hopf bifurcation.

2.3 A cell cycle reduced model

The reduced model of the mammalian cell cycle developed by Almeida et al. (2017) is a system of two variables: MPF (*mitosis promoting factor*) which is a cyclin-Cdk complex that phosphorylates multiple proteins during mitosis phase, and APC:cdc20, (subunit of the *anaphase-promoting complex*) which is a large complex of proteins that promote exit from mitosis phases through MPF and other kinases degradation. The network consists of an activator (MPF) and an inhibitor (APC:cdc20), both of them crucial components of cell division. This two-variable model was calibrated from experimental data, Pomerening et al. (2005) and shown to reproduce the observations in a very reasonable way. The two dimensional model is as follows:

$$
\begin{aligned}
\frac{d[APC:cdc20]}{dt} &= V_m[MPF] - V_k[APC:cdc20] \\
\frac{d[MPF]}{dt} &= S_{GF} + V_c \frac{\overline{MPF_{max}} - [MPF]}{\overline{MPF_{max}} - [MPF] + k_c} \frac{[MPF]^m}{[MPF]^m + k_m^m} \\
&\quad - V_w \frac{[MPF]}{[MPF] + k_w} \frac{k_n^n}{[MPF]^n + k_n^n} \\
&\quad - \gamma_1 [APC:cdc20][MPF],
\end{aligned}
$$

with parameters given in Table 2. Very briefly, the constant S_{GF} represents growth factor, the term in V_c represents the positive feedback loop involving cdc25, while the term in V_w represents the double negative loop involving wee1.

Table 2: Parameters of cell cycle model

$V_m = 0.0168\ min^{-1}$	$V_k = 0.0107\ min^{-1}$
$S_{GF} = 5.6917\ min^{-1}$	$V_c = 225.71\ min^{-1}$
$V_w = 747.61\ min^{-1}$	$\overline{MPF_{max}} = 284.1087$
$k_c = 130.3331$	$k_m = 98.5219$
$k_w = 137.9830$	$k_n = 0.1164$
$\gamma_1 = 0.0162\ min^{-1}$	$m, n = 2$

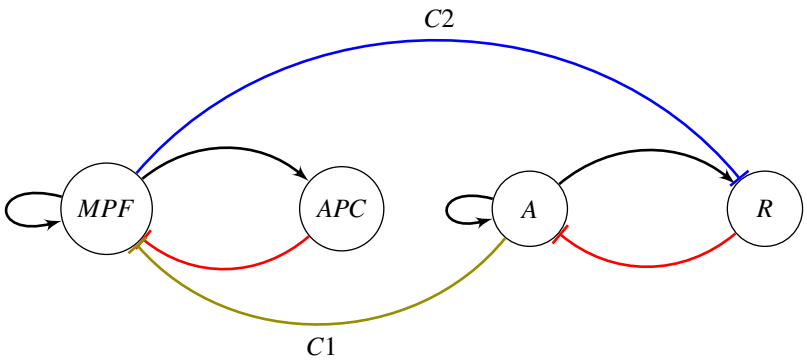

Figure 3: Cell cycle and Smolen oscillator coupled network

3 Interactions between the two oscillators

In mammalians, it is known that the circadian clock affects the cell cycle, and more recently there has been evidence that the cell cycle may also directly affect the clock Feillet et al. (2014). Thus, in addition to their specific characteristics as biological processes, a very important aspect to be studied is their interaction: in some tissues, the pace with which the cell divides into two daughter cells (*mitosis phase*) is regulated by the cell circadian clock, Feillet et al. (2014), Ünsal-Kaçmaz et al. (2005). More precisely, the regulation of one specific kinase-inhibitor of the cell cycle,*Wee1*, by the clock genes, has been observed and explains the circadian control of cell cycle division Gérard and Goldbeter (2012), Matsuo et al. (2003).

3.1 A scheme for bidirectional coupling

To model the interaction from the circadian clock to the cell cycle we have that: the activator A in the Smolen model, that stands for the complex CLOCK/BMAL1, influences the cell cycle through activation of the kinase Wee1 that inhibits MPF, Gérard and Goldbeter (2012) , Matsuo et al. (2003).

The influence of the cell cycle on the clock is less clear, but an hypothesis is that of Feillet et al. (2015): the protein MPF inhibits the nuclear receptor REV-ERBα that is assumed as the component R (repressor) of the Smolen oscillator. We mention that there is no specific evidence on the form of clock regulation by the cell cycle, see in Feillet et al. (2015), so our current study will explore several possibilities for coupling schemes. A general scheme for bidirectional coupling between the two oscillators is shown in Fig. 3.

3.2 Period - response analysis

To better analyse the period response of the coupled system, and to identify whether either of the oscillators has a dominant contribution, we develop the following criteria.

We characterize the two systems as controller and follower comparing the 3 period values, the cell cycle period T_{cc}, the Smolen oscillator period T_{Smolen} and the coupled system period T_{bi}. Then define:

Definition 1 *Let* $T_{min} = min\{T_{cc}, T_{Smolen}, T_{bi}\}$, $T_{max} = max\{T_{cc}, T_{Smolen}, T_{bi}\}$ *and* T_{int} *be the intermediate of the three period values. Then the controller is defined to be the oscillator with the period closer to that of the coupled system:*

(a) If $T_{bi} = T_{min}$ *or* $T_{bi} = T_{int}$ *and*

$$\frac{T_{bi}}{T_{max}} \ll min\left\{\frac{T_{bi}}{T_{int}}, \frac{T_{min}}{T_{bi}}\right\}$$

then the controller is the oscillator with lower period.

(b) If $T_{bi} = T_{min}$ *or* $T_{bi} = T_{int}$ *and*

$$\frac{T_{bi}}{T_{max}} \gg max\left\{\frac{T_{bi}}{T_{int}}, \frac{T_{min}}{T_{bi}}\right\}$$

then the controller is the oscillator with higher period.

(c) If $T_{bi} = T_{max}$ *and* $\frac{T_{int}}{T_{max}} \approx 1$ *then the controller is the oscillator with higher period.*

(d) If $T_{bi} = T_{min}$ *or* $T_{bi} = T_{int}$ *and*

$$\left|\frac{T_{min}}{T_{int}} - \frac{T_{min}}{T_{max}}\right| < \varepsilon \text{ or } \left|\frac{T_{min}}{T_{int}} - \frac{T_{int}}{T_{max}}\right| < \varepsilon$$

for $\varepsilon = 0.1$*, then no oscillator is considered as controller.*

4 Two coupling mechanisms

Following the discussion in Section 4, we investigate two general cases: the oscillators affect each other through synthesis or through degradation rates.

4.1 Coupling through synthesis rate

First, we consider the case where the clock acts on the cyclin complex MPF synthesis rate, i.e. BMAL1/CLOCK modulates parameter V_c, which expresses the activation of the kinase cdc25. The coupling is expressed through a saturation function:

$$C1 = v_1 \frac{\delta_1}{\delta_1 + A} \tag{3}$$

where δ_1 represents the coupling strength and v_1 guarantees that the concentrations remain at sufficient levels. The term $C1$ multiplies V_c.

Conversely, the complex MPF acts on REV-ERBα synthesis rate by inhibition:

$$C2 = v_2 \frac{\delta_2}{\delta_2 + MPF} \tag{4}$$

The term $C2$ multiplies V_R in (2).

We study the interaction between the two oscillators as a function of the coupling strength. First, our results show that, through bidirectional coupling the two oscillators lock at phase 1:1. Second, varying the coupling parameters, the clock tends to play the role of controller, see Fig. 5, top. Indicatively, for v_1, $v_2 = 1.2$, and for coupling strengths $\delta_1 = 0.5$ and $\delta_2 = 100$, (corresponding to 0.14 % of the maximum value of A and 91.65 % of the maximum value of MPF in the uncoupled systems), there is strong effect from the clock and weaker from the cell cycle : $\frac{T_{bi}}{T_{cc}} = 0.22$ while $\frac{T_{bi}}{T_{Smolen}} = 0.92$.

4.2 Coupling through degradation

We now investigate the case where the clock acts directly on the degradation rate of the MPF component of the cell cycle. The coupling term now is expressed through an increasing function since A promotes degradation rate of MPF:

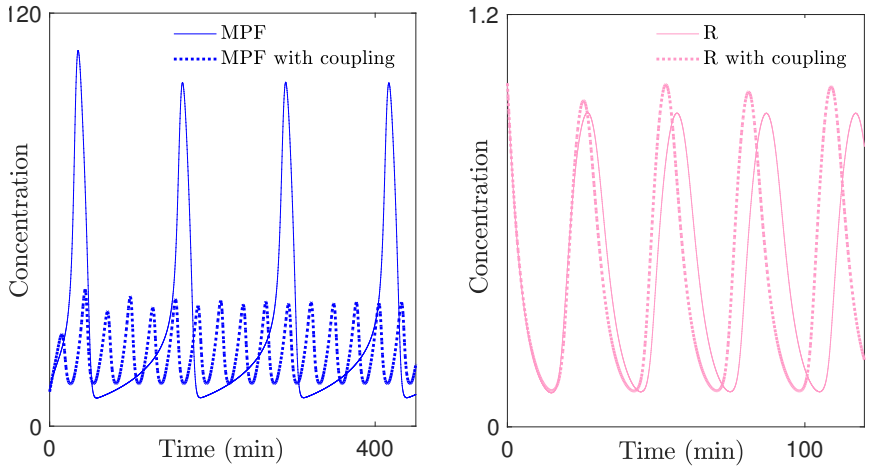

Figure 4: Activity of variables MPF (cell cycle) and R (clock), with or without couplig (respectively, solid and dashed lines). Strong coupling from the side of the clock, initial period $T_{Smolen} = 30$ min, $T_{cc} = 126.77$ min, period of the coupled system: $T_{bi} = 27.78$ min. Coupling parameters used: v_1, $v_2 = 1.5$, $\delta_1 = 1.5$, $\delta_2 = 100$.

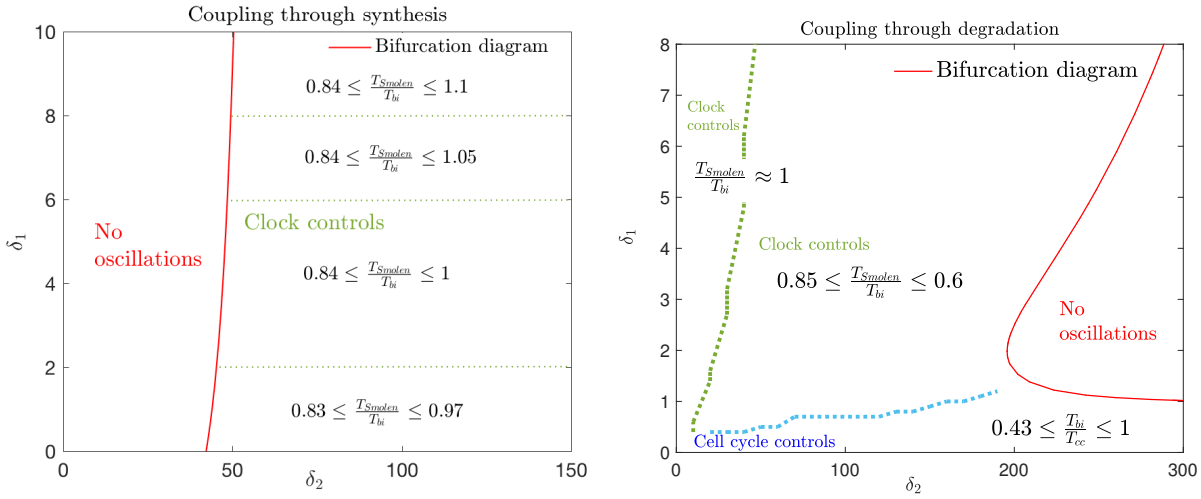

Figure 5: Coupled system period - response in the two interaction cases, as the coupling strengths δ_1, δ_2 vary. Remaining parameters used: see Table 1 for the Smolen model, Table 2 for the cell cycle, v_1,v_2 =1.

$$C1 = v_1 \frac{A}{\delta_1 + A} \tag{5}$$

This function will multiply the term $-\gamma_1$APC MPF, in MPF equation of cell cycle model.
Likewise, MPF now promotes the degradation rate of the REV/ERB-α. The coupling term will be:

$$C2 = v_2 \frac{MPF}{\delta_2 + MPF} \tag{6}$$

The term C2 will multiply the degradation rate $-\gamma_R$ R, in R equation of the Smolen model, see (2). This scheme of interactions allows a wider range of period responses, as illustrated in Fig. 5, bottom. For instance, we now present a case where both oscillators strongly contribute to the coupling. With coupling parameters v_1, $v_2 = 1$, $\delta_1 = 0.5$, $\delta_2 = 100$ and uncoupled periods $T_{Smolen} = 30$ min, $T_{cc} = 126.77$ min, the period of the coupled system is $T_{bi} = 63.68$ min, with ratios: $\frac{T_{bi}}{T_{cc}} = 0.5$ and $\frac{T_{Smolen}}{T_{bi}} = 0.43$. Two ratios are very close so, according to Definition 3.2, none of the oscillators is a controller.

4.3 Controller - follower results

We are interested in exploring the coupling parameter range for which the two systems play the roles controller - follower. In Fig. 5 top, for the first interaction case (coupling through synthesis), we see that varying the coupling strength from the side of clock δ_1, the period of the coupled system stays close to that of the clock. Thus, according to Definition 3.2, the clock is the controller in this case.

We also observe that δ_2 (cell cycle $\rightarrow$ clock) does not greatly affect the qualitive period response. Whereas in the case of interaction through degradation rate (Fig. 5, bottom), the coupled system period varies with both δ_1 and δ_2. To interpret the controller - follower results in both coupling cases, we extract information from the bifurcation analysis for the synthesis and degradation parameters of the two systems. (Bifurcation analysis performed using Matcont.)

Cell cycle controls In the case of coupling through degradation the cell cycle is able to play the role of the controller, as δ_2 increases and δ_1 remains low. This result can be interpreted as a stronger action from the cell cycle on the coupling: $\delta_1 \leq 0.5$, is less than the minimum concentration value of the uncoupled A and $\delta_2 \leq 109.1$ lower than the maximum uncoupled MPF, so it is likely that the term C_2 (6) contributes to significantly decrease the degradation rate of R. The latter results in the decrease of concentration of A, which finally can only weakly inhibit the cell cycle through MPF. In a simplified way, weak action from the side of clock allows the cell cycle to control the coupled system period; indicatively, our results show $\frac{T_{bi}}{T_{cc}} \approx 1$, for $\delta_2 = 100$ and $0.2 < \delta_1 \leq 0.5$.

For a deeper analysis of this scenario, we extract information from the bifurcation analysis for the synthesis and degradation parameters of the uncoupled Smolen system. In Fig. 6 right we indicate the parameter region where the uncoupled Smolen oscillates. We note that for the initial $V_A = 12.5\ min^{-1}$ the system becomes stable for $\gamma_R < 0.077\ min^{-1}$. Hence, as the coupling strength δ_2 from the side of cell cycle increases the term $-\gamma_R C_2$ decreases and the system has no longer periodic solutions. The cell cycle in this case is able to play the role of the controller when the Smolen system is close to exit the oscillatory region. For instance, if $\delta_2 = 80$ ($\delta_1 = 0.5$), we have that $-\gamma_R C_2 < 0.14$ and $\frac{T_{bi}}{T_{cc}} = 0.8$, see Fig. 7 (bottom).

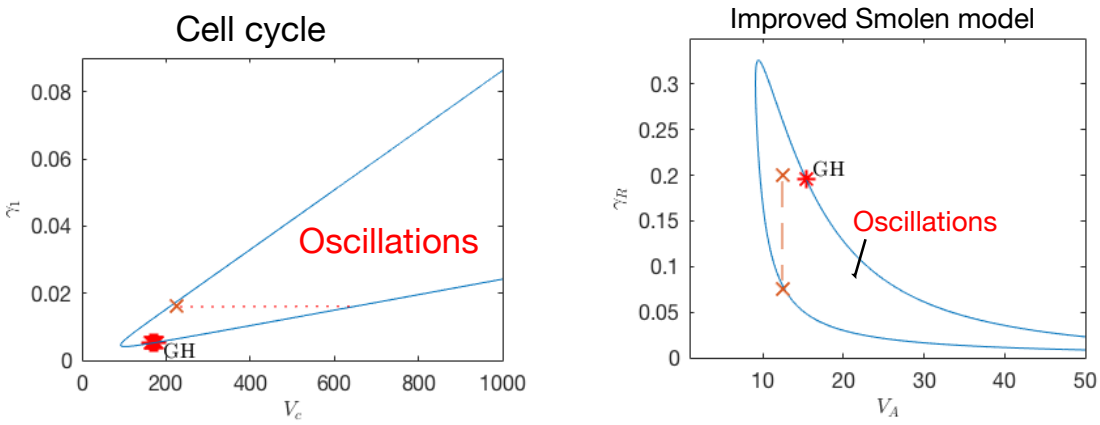

Figure 6: Bifurcation analysis for cell cycle synthesis and degradation parameters (left) and the improved Smolen model (right). The red stars indicate Generalized Hopf points.

Clock controls As we observe in Fig.6 (left) the uncoupled cell cycle becomes stable for $\gamma_1 < 6.4 \times 10^{-3}$ if $V_c = 225.71\ min^{-1}$. In the case of coupling through degradation, the term C_1 (5) becomes very small as δ_1 increases, (Fig. 7 top), thus it forces the cell cycle to become stable: for $\delta_1 > 1$, ($\delta_2 = 100$) we have that $-\gamma_1 C_1 < 5 \times 10^{-3}$. Under these coupling parameter conditions, clock is the controller with $\frac{T_{bi}}{T_{Smolen}} \geq 0.7$, Fig. 5 bottom. This observation can be interpreted as: the clock is more likely to be the controller of the coupled system period when the cell cycle starts to loose its instability due to the coupling strength.

In the case of coupling through MPF synthesis rate the cell cycle looses instability much faster than in the case of degradation: the initial γ_1 value is $0.0162\ min^{-1}$ and for $V_c < 210\ min^{-1}$ system (3) has no longer periodic behavior, see the bifurcation analysis in Fig. 6 left. Since the initial V_c value is $225.71\ min^{-1}$ the term $V_c C_1$ decreases immediately as δ_1 increases, C_1 as in (3). One can translate this behavior as a strong clock effect on the coupled system period response, in this case (Fig. 5 top).

4.4 Effect of synthesis rates parameters

We now investigate the effect on the coupled system period of varying each oscillator period. This is done separately by varying the synthesis rate parameters V_c of MPF and V_A of A.

In Fig. 8 (top), we observe that increasing V_c the coupled system period remains constant for both interaction cases. However, in the case of coupling through degradation, the coupled system period is greater than in case of coupling through synthesis. An interesting observation is that even when the cell cycle is at a stable steady state (for $V_c < 209\ min^{-1}$), the coupled system manifests oscillations in both interaction cases.

Varying now the synthesis rate of A (at bottom of Fig. 8), we notice that for $V_A > 12\ min^{-1}$ the uncoupled clock period increases and so does the coupled period. The latter is strongly controlled by the clock when the coupling is through synthesis rate. In the case where the coupling is through degradation rate, T_{bi} takes higher values reflecting the cell cycle contribution.

It is surprising though, that for $V_A > 15.5\ min^{-1}$ the clock (Smolen system) is at a stable steady state, whereas the coupled system oscillates with period around 50 min. In this way the cell cycle forces the clock (Smolen system) to oscillate. This observation can be interpreted as the capacity of the cell cycle to induce oscillations of the coupled system even when the clock is at a steady state.

In the bifurcation diagram for the parameters V_A, γ_R of Fig. 6 we observe that as γ_R reaches values lower than $0.02\ min^{-1}$ the interval for periodic solutions of V_A shifts to the right and increases. Indeed,

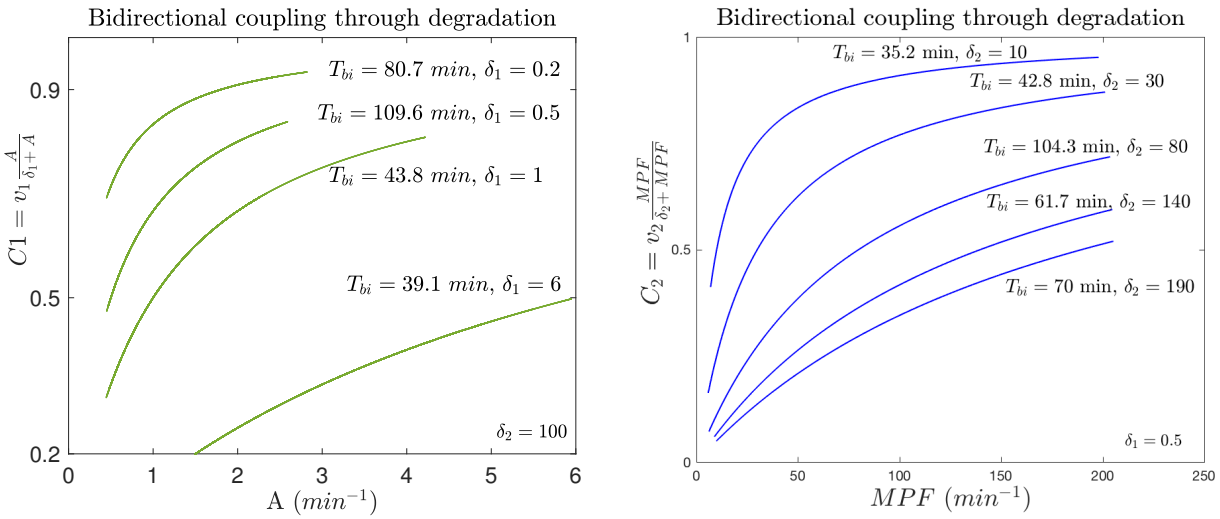

Figure 7: The term C_1 in coupling through degradation, as a function of the activator A concentration amplitude (top) v_1, $v_2 = 1$, $\delta_2 = 100$. The term C_2 in coupling through degradation, as a function of MPF concentration amplitude (bottom) v_1, $v_2 = 1$, $\delta_1 = 0.5$.

with coupling through degradation rate, the term $-\gamma_R C_2$ decreases as δ_2 increases, see Fig. 7 bottom, C_2 as in (6). For example, for $\delta_1 = 1$ and $\delta_2 = 100 \Rightarrow 0.05 < -\gamma_R C_2 < 0.7$, so R degradation rate decreases allowing V_A to take higher values in the oscillatory region, see Fig. 6 right. Thus, although the uncoupled Smolen system is at a stable steady state, the coupled system oscillates as it is shown in Fig. 8 (bottom).

5 Conclusion

In this paper we present a model-based investigation of the cell cycle and circadian clock coupling, using two reduced models. We consider two bidirectional schemes for the coupled system and observe that: (i) generally, in the case of coupling through synthesis rates, the coupled system closely follows the clock period, (ii) in the case of coupling through degradation rates, the cell cycle may have a higher contribution on the coupling. In either scheme, it is interesting to note that each of the oscillators can alone induce oscillations in the coupled system, implying that the coupling contributes to increase the parameter region where oscillations happen.

Many different coupling schemes remain to be discussed and tested. However, the current analysis provides some indications on how to couple the two systems so that the joint periodic behavior is improved and also suggests ways of regulating the period of the coupled system through one of the oscillators. These are promising directions to consider in the context of synthetic biology.

References

Almeida, S., Chaves, M., Delaunay, F., and Feillet, C. (2017). A comprehensive reduced model of the mammalian cell cycle. *IFAC-PapersOnLine*, 10.1016/j.ifacol.2017.08.2204.

Dhooge, A., Govaerts, W., and Kuznetsov, Y. (2003). Matcont: a matlab package for numerical bifurcation analysis of odes. *ACM Trans. Math. Softw.*, 10.1145/980175.980184.

Elowitz, M.B. and Leibler, S. (2000). A synthetic oscillatory network of transcriptional regulators. *Nature*, 403(6767), 335–338.

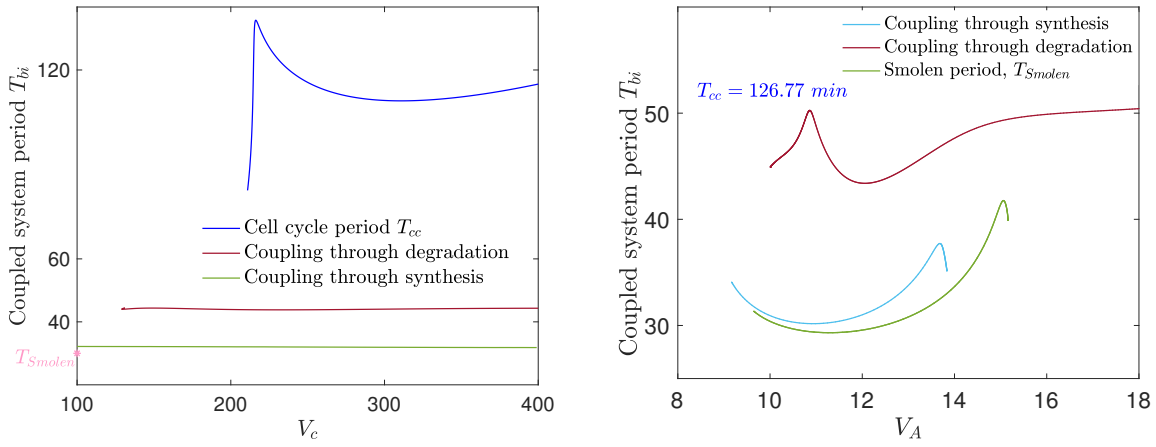

Figure 8: Coupled system period as a function of V_c (synthesis rate of MPF) and V_A (synthesis rate of A, bottom) in the two interaction cases. Coupling parameters used: v_1, $v_2 = 1$, $\delta_1 = 1$, $\delta_2 = 100$.

Feillet, C., Krusche, P., Tamanini, F., Janssens, R.C., Downey, M.J., Martin, P., Teboul, M., Saito, S., Lévi, F.A., Bretschneider, T., van der Horst, G.T.J., Delaunay, F., and Rand, D.A. (2014). Phase locking and multiple oscillating attractors for the coupled mammalian clock and cell cycle. *Proceedings of the National Academy of Sciences of the United States of America*, 10.1073/pnas.1320474111.

Feillet, C., van der Horst, G.T.J., Levi, F., Rand, D.A., and Delaunay, F. (2015). Coupling between the circadian clock and cell cycle oscillators: Implication for healthy cells and malignant growth. *Frontiers in Neurology*, 10.3389/fneur.2015.00096.

Firippi, E. and Chaves, M. (In preparation). Improving the design of a synthetic genetic oscillator by piecewise linear approximation.

Gérard, C. and Goldbeter, A. (2012). Entrainment of the mammalian cell cycle by the circadian clock: Modeling two coupled cellular rhythms. *PLoS Computational Biology*, 10.1371/journal.pcbi.1002516.

Glass, L. and Kauffman, S.A. (1973). The logical analysis of continuous, non-linear biochemical control networks. *Journal of Theoretical Biology*, https://doi.org/10.1016/0022-5193(73)90208-7.

Matsuo, T., Yamaguchi, S., Mitsui, S., Emi, A., Shimoda, F., and Okamura, H. (2003). Control mechanism of the circadian clock for timing of cell division in vivo. *Science*, 10.1126/science.1086271.

Perez-Carrasco, R., Barnes, C.P., Schaerli, Y., Isalan, M., Briscoe, J., and Page, K.M. (2018). Combining a toggle switch and a repressilator within the ac-dc circuit generates distinct dynamical behaviors. *Cell Systems*, 10.1016/j.cels.2018.02.008.

Pomerening, J.R., Kim, S.Y., and Ferrell, J.E. (2005). Systems-level dissection of the cell-cycle oscillator: Bypassing positive feedback produces damped oscillations. *Cell*, 122, 565–578.

Purcell, O., Savery, N.J., Grierson, C.S., and di Bernardo, M. (2010). A comparative analysis of synthetic genetic oscillators. *J R Soc Interface*, 10.1098/rsif.2010.0183.

Smolen, P., Baxter, D.A., and Byrne, J.H. (1998). Frequency selectivity, multistability, and oscillations emerge from models of genetic regulatory systems. *American Journal of Physiology - Cell Physiology*, 274(2), C531–C542.

Stricker, J., Cookson, S., Bennett, M.R., Mather, W.H., Tsimring, L.S., and Hasty, J. (2008). A fast, robust and tunable synthetic gene oscillator. *Nature*, 10.1038/nature07389.

Tomazou, M., Barahona, M., Polizzi, K.M., and Stan, G.B. (2018). Computational re-design of synthetic genetic oscillators for independent amplitude and frequency modulation. *Cell Systems*, https://doi.org/10.1016/j.cels.2018.03.013.

Ünsal-Kaçmaz, K., Mullen, T.E., Kaufmann, W.K., and Sancar, A. (2005). Coupling of human circadian and cell cycles by the timeless protein. *Molecular and Cellular Biology*, 25(8), 3109–3116.

Ye, R., Selby, C.P., Chiou, Y.Y., Ozkan-Dagliyan, I., Gaddameedhi, S., and Sancar, A. (2014). Dual modes of clock:bmal1 inhibition mediated by cryptochrome and period proteins in the mammalian circadian clock. *Genes & development*, 10.1101/gad.249417.114.